IEEE Access
Multidisciplinary | Rapid Review | Open Access Journal

Received June 20, 2021, accepted August 8, 2021, date of publication August 11, 2021, date of current version August 19, 2021.

Digital Object Identifier 10.1109/ACCESS.2021.3104167

Global Electricity Interconnection With 100% Renewable Energy Generation

CONG WU, XIAO-PING ZHANG, (Fellow, IEEE), AND MICHAEL J. H. STERLING

Birmingham Energy Institute, University of Birmingham, Birmingham B15 2TT, U.K.
Department of Electronic, Electrical and Systems Engineering, School of Engineering, University of Birmingham, Birmingham B15 2TT, U.K.

Corresponding author: Xiao-Ping Zhang (x.p.zhang@bham.ac.uk)

This work was supported in part by the Engineering and Physical Sciences Research Council (EPSRC) under Grant EP/N032888/1 and Grant EP/L017725/1.

ABSTRACT Under the United Nations 'Net-Zero 2050' target, transition towards a 100% renewable energy (RE) sourced power grid has become an ever more attractive pathway. However, the inherent fluctuations and intermittency of RE generation, particularly wind and solar, would inevitably pose great technical and economic barriers to their massive integration into the energy supply. A global interconnected electricity grid to utilize the complementarity of diverse demand patterns and RE sources provides an appealing solution. With detailed datasets, this paper is therefore to assess the economic benefits of such a global electricity grid with 100% RE generation using the state-of-the-art Ultra High Voltage Direct Current transmission technologies. The global electricity grid is split into 14 regions with 20 potential interconnection routes and regional geographical centroid is treated as equivalent node for inter-regional distance calculation. Global hourly meteorological re-analysis data of up to seven years with spatial resolution of $0.25^\circ \times 0.25^\circ$ (approximate 28km $\times$ 28km) is used to generate regional representative generation power series. With the minimum annual system cost for meeting demand in 2050, an integrated planning and power dispatch model is presented to determine the additional regional capacities of RE sources, storage systems, and the interconnectors from 2030, and in which load curtailment is incorporated and 'N-1' security are much stricter than those traditionally applied. The paper provides a comprehensive analysis with 24 cases based on different supply portfolios which show a 20% cost saving through specific global interconnections thereby lending support to the concept of a Global Electricity Grid.

INDEX TERMS Ultra high voltage direct current (UHVDC), high voltage direct current (HVDC), renewable energy, solar generation, wind generation, hydropower generation, energy storage, load curtailment, global electricity interconnection, global electricity grid, net zero, power system security, power system planning.

I. INTRODUCTION

A policy target of net-zero emissions of greenhouse gases, inevitably means a high proportion of renewable energy (RE) is to be anticipated in future global energy system [1]–[4], particularly the electricity systems. However, power from RE sources like solar and wind inherently shows strong fluctuation and intermittency, which poses great challenges to system stability and significantly increases the balancing costs. Complementarity of RE sources [5], [6], storage systems [7], sector coupling [8], [9], and grid extension [10] can potentially mitigate such variability. Ultra-high voltage (UHV) transmission [11]–[13] has raised the prospect of long distance transcontinental electricity interconnection [14], [15] to utilize complementary effects of diverse RE resources and demand patterns in a wide geographical scale. Hence the investigations on the economic benefits of such electricity interconnections and even global electricity interconnection to support high or even 100% RE penetration would be of great interest.

In the past, there have been studies on electricity interconnections between regions. Plans for connecting Europe to Russia for importing onshore wind/hydro energy and to the Mediterranean region for importing desert solar energy were explored respectively [16], [17]. Potential routes for interconnection between Europe with China [18] and with Central Asia [19] were presented by the Joint Research Centre (JRC) of the European Commission and the benefits of

The associate editor coordinating the review of this manuscript and approving it for publication was Feng Wu.

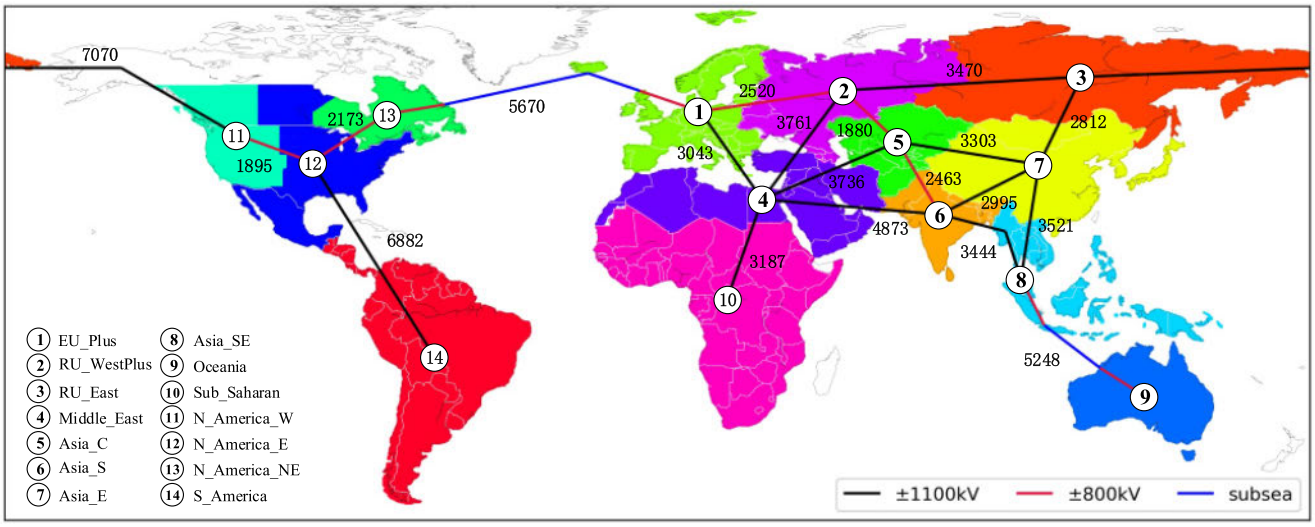

FIGURE 1. Global electricity grid with 14 regions and 20 potential interconnection routes.

connected Europe and North America was further analyzed in depth [20]. Grid interconnection schemes among Xinjiang in China, Pakistan in southern Asia and five central Asian countries as well as Arab countries are explored in [21] and [22]. An organization called GEIDCO proposed their global backbone grid scenarios [23] together with detailed regional schemes, e.g. North America [24] and the 'EuroAsia interconnector' is already under construction to link Israel to Greece through Cyprus [25]. The value of increased HVDC capacity between East and West power grids in US were also recently investigated under a project called 'Interconnections Seam Study' by National Renewable Energy Laboratory (NREL) [26].

The idea of global electricity interconnection can be traced back to early 1980s [27] and has enjoyed a rapidly growing attention recent years in a context of accommodating high-share RE as well as the technology breakthrough of UHV DC transmission. An organization called GEIDCO proposed their global backbone grid scenarios [23] together with detailed regional schemes, e.g. North America [24]. The benefits and challenges of global power grids were comprehensively reviewed in [28]. Recently, the feasibility of global electricity network structured in 13 regions was studied by CIGRE Working Group C1.35 [29]. In the above works, there has been a lack of either detailed models or high granularity of demand and generation data, nor has 100% RE generation been adequately considered yet.

The latest status and perspectives on 100% RE systems have been reviewed in [30] and an interconnected European electricity system based on 100% RE supply was presented respectively in [31] and [32] using one-year weather data with a spatial resolution of $0.3125° \times 0.3125°$ and $0.75° \times 0.75°$, where the model was run for a full year with hourly resolution. Similar weather-driven planning model with data spatial resolution of $0.45° \times 0.45°$ was applied to optimize the portfolios of energy technologies in North-East Asia [33] and America [34], where regional interconnection is taken into consideration. The role of inter-provincial transmission is investigated in a fully renewable Chinese power system [35], [36]. Most recently, a 100% renewable US power system using gigawatt-scale solar, wind, existing hydropower, lithium-ion batteries, and transmission were modelled, showing inter-state coordination yield a cost reduction of 46% [37]. However, these works on 100% RE supply have been limited to the national, regional, continental level electricity interconnection. In [38], 3-region interconnections between Europe, North-East Asia, and North America with 100% renewable generation were studied very recently.

From the perspectives of implementing global 'Net-Zero', the power grid interconnection for exploring the complementarity, diversity and availability of RE sources globally becomes an attractive pathway, and hence this paper is focused on global electricity interconnection with 100% RE supply and investigates whether such a grid can bring economic benefits by utilizing the complementary effects of diverse resources in a global scale. The novel contributions of this paper are as follows:

- A detailed global electricity grid with 14 regions and 20 potential routes: The global power grid is split into 14 regions with 20 potential routes, and respective geographical centroid is treated as regional equivalent node and used for inter-regional distance calculation. Regions, potential routes and interconnector length are shown in Fig. 1.
- Detailed hourly demand and generation data series for 14-region global electricity grid for 12 months: Global hourly meteorological re-analysis data of up to seven years with spatial resolution of $0.25° \times 0.25°$ is converted into solar, onshore, and offshore wind power series respectively, leading to a total of 224,750 grid cells for land areas and 19,958 grid cells for marine

areas. Hourly generation within those cells are selected, aggregated, and further clustered into one year regional series based on weight-based aggregation rules and density-based cluster algorithms.
- A more accurate method for determining the physical distances between the centers of 14 regions: Regarding the distance between two points on the Earth, a Python package called 'pyproj' is adopted to determine the physical distance between two regions.
- Optimal planning model of the global electricity grid to explore the complementarity of diverse demand patterns and RE sources globally: With minimum annual system cost of the whole 14-region global grid whose demands in 2050 are expected to be met by 100% RE, i.e., wind, solar, hydropower, energy storage, a co-optimized planning and dispatch model is presented to determine the additional capacities of RE technologies, electricity storage systems, and the interconnectors since 2030, where load curtailment and 'N-1' security of interconnectors is are considered.

This paper is structured as follows. Section II proposes the procedure to generate regional power series of RE and demand as well as some key parameters. Section III deals with the problem formulation, a co-optimized capacity planning and dispatch model is constructed to determine the capacities of RE sources, storage systems and the interconnectors where load curtailment as well as 'N-1' security of interconnectors are considered. Section IV shows the numerical results and comparative analysis, followed by the conclusions in Section V.

II. BASIC SYSTEM DATA AND PARAMETERS

In this study, four generating technologies together with storage system are employed to power the grid, namely onshore wind, offshore wind, solar PV, and hydro, which are commonly recognized as important energy sources in different independent research groups [2], [4], [32], [37]. For conventional thermal generators, the input is considered to be stable and thus the production output is mainly restricted to its capacity when dispatched, but for weather-driven generating technologies, e.g., wind and solar, its output is additionally limited to instantaneous wind strength or solar insolation. It is therefore necessary to obtain the hourly available power of solar and wind generation. Regional demand and hydro series, as well as information about interconnections between regions are key inputs as well.

All the time series of regional demand and RE power are expressed as UTC+00. All the data processing is coded with Python on an IntelCore-i5-8300H/2.3GHz personal laptop with 8G memory.

A. HOURLY SOLAR AND WIND POWER SERIES

Historical meteorological re-analysis data of up to seven years (2011 $\sim$ 2017) with spatial resolution (longitude $\times$ latitude) of 0.25° $\times$ 0.25°(approximate 28km $\times$ 28km) and temporal resolution of one hour are converted into solar and wind power series based on a similar method to that proposed in [39] using an open-source Python package called 'Atlite' and widely used in [32], [35], [36], [40].

There are a total of 224,750 grid cells for land areas and 19,958 grid cells for marine areas. The meteorological data takes up a storage space of some 5Terabytes (TB). Due to the large amounts of data involved, it is worth noting that the downloading of the 7-year hourly weather data took more than one month and a further 160 hours was taken to convert the weather data into onshore wind, offshore wind and solar power series.

1) HOURLY WEATHER DATASETS

A meteorological dataset called 'ERA5' is employed, which is produced by the European Centre for Medium-Range Weather Forecasts (ECMWF) [36]. The water depth of the marine area is obtained from the General Bathymetric Chart of the Oceans (GEBCO) [37] and National Centers for Environmental Information (NCEI) [38]. The geographical shape files of administrative boundaries are retrieved from Natural Earth Dataset [39] for country shapes and the Database of Global Administrative Areas (GADM) [40] provides different layers of boundaries within each country.

It should be noted that the dataset is downloaded for each sub-region instead of the entire region, specifically, country level is the minimum scale for regions except for Russia, Canada, China, and the US where provinces and states are the minimum scale.

2) CONVERTING AND AGGREGATING OF SOLAR AND WIND DATA

It is assumed that an equivalent 1-MW wind turbine and 1-MW PV panel are placed in the center of each raster cell. The meteorological data are then converted to hourly power series for each cell.

The Enercon E-101 model of a wind turbine with rated capacity of 3050kW and 150m hub height is used to generate onshore power series whose power curves can be obtained from the wind turbine repository at an open platform [41] and the NREL Reference Turbine with 5 MW at 90 m is employed to generate offshore power series. The original power curve is further improved to account for the smoothing effects of wind speed within each cell by Gaussian kernel [39]. The wind speed at height of 100 m provided in the dataset is extrapolated to that of 150m using a logarithmic method with roughness [39].

A CdTe-based PV model with fixed tilt angle optimized by the grid cell's latitude is chosen to generate solar power series. An optimal tilt angle for the given latitude is obtained using a simple method [42] which works for latitudes between 0 and 50 and returns a static 40 degree angle for higher latitudes where the angle may not be that important [43], [44]. The fitted model of CdTe solar panel was presented by Huld [45] to estimate the energy yield of PV modules based on irradiance and temperature. This function in 'Atlite' is adapted from

TABLE 1. Regional capacity factors (%).

Region	Solar		Onshore		Offshore		Hydro
	7 years	Rep.	7 years	Rep.	7 years	Rep.	2019
EU_Plus	15.53	15.50	33.54	33.34	51.20	50.69	36.11
RU_WestPlus	13.19	13.14	41.77	41.63	48.95	48.93	43.21
RU_East	14.12	14.12	34.30	34.43	42.47	43.38	43.21
Middle_East	24.55	24.57	35.34	35.27	33.60	33.55	30.25
Asia_C	20.54	20.57	38.72	38.75	0.00	0.00	34.36
Asia_S	22.14	22.22	21.84	22.22	30.73	30.97	41.23
Asia_E	20.91	20.87	26.83	26.67	40.56	40.09	40.10
Asia_SE	18.94	19.00	10.67	10.74	20.37	20.14	34.73
Oceania	22.88	22.76	43.18	43.53	43.60	43.49	35.28
Sub_Saharan	23.13	23.13	29.41	29.50	25.65	25.64	39.25
N_America_W	20.73	20.74	27.33	27.51	37.34	36.76	43.44
N_America_E	20.20	20.05	35.58	36.06	37.75	37.25	46.64
N_America_NE	15.24	15.42	49.23	48.99	52.98	52.91	55.63
S_America	21.19	21.09	23.96	23.86	44.30	44.26	46.83

another python package called 'GSEE' [46]. Details about wind and solar converting model are shown in [40].

The converted power series are further aggregated from raster cell level to sub-region level using (1) based on the assumption that $0 \sim 10\%$ and $10\% \sim 20\%$ of the raster cells with highest average capacity factor (CF) are weighted by 0.3, $20\% \sim 30\%$ of the cells with highest CF are weighted by 0.2, and last $30\% \sim 40\%$ and $40\% \sim 50\%$ of the cells with highest CF are weighted by 0.1 [34]. This indicates that generation sites are scattered on 50% of the geographical area within each sub-region.

$$cf^S_{r,s,j,t} = \sum_{i=1}^{5} w^S_i (p_{r,s,j,i,t}/c_{r,s,j,i}), \quad t \in [1, 61320] \quad (1)$$

where $p_{r,s,j,i,t}$ is the aggregated power of group i in sub-region s within region r at hour t for RE type j and $c_{r,s,j,i}$ is the aggregated capacity. w^S_i is the weight of group i and $cf^S_{r,s,j,t}$ represents equivalent CF series of RE type j in sub-area s within region r.

Henceforth, the expression of 'power series' actually means 'CF series' which directly indicates the hourly available output of RE generation under given capacity.

3) POTENTIAL OF RE GENERATION WITHIN A SUB-REGION

The installing potential of solar PV, onshore wind and offshore wind within a sub-region is related to the usable land area and installation density, shown in (2).

$$C_{r,s,j} = A_{r,s,j} D_j \quad (2)$$

where $A_{s,j}$ is the share of usable land allowed for installing RE technology j in sub-region s of region r, D_i is the installation density of RE technology j and $C_{r,s,j}$ therefore denotes the maximum capacity.

It is assumed for all sub-regions that up to 6% of the land area can be covered by PV cells while only 4% allowed for onshore wind farms due to the societal constraints [4]; a share of 10% of the marine area can be covered by offshore wind farms. The installation density of onshore, offshore wind turbines, and PV modules are assumed to be 10 MW/km^2, 10 MW/km^2, and 81.8 MW/km^2, respectively [2], [36]. Besides, sites with a maximum water depth of 50 meters are selected to install offshore wind turbines [31], [32].

4) REGIONAL POWER SERIES OF SOLAR AND WIND

The equivalent regional power series for RE type j in this study are calculated by the weighted sum of equivalent power (CF) series of each sub-region using (3).

$$cf^R_{r,j,t} = \sum_{s=1}^{N_r} w^R_{r,s,j} cf^S_{r,s,j,t} \quad t \in [1, 61320] \quad (3)$$

where $w^R_{r,s,j}$ denotes the weight for power series of RE type j in sub-region s within region r, expressed as the installing potential of sub-area s over the total potential in region r and calculated as (4); $cf^R_{r,j,t}$ is the calculated equivalent CF series of RE type j in region r that consists of N_r sub-regions.

$$w^R_{r,s,j} = C_{r,s,j} / \sum_{s=1}^{N_r} C_{r,s,j} \quad (4)$$

5) REPRESENTATIVE POWER SERIES OF SOLAR AND WIND

For each region, a four-week long hourly power series commencing Monday is sampled from seven-year regional time series and further grouped for each month. For example, there are 7 pieces of four-week time series for solar PV in January of during 7 years. Therefore, 12 month sets are formed, each of which comprises of 7 elements.

Furthermore, a popular density-based clustering method, named DBSCAN [47], is applied to select one representative time series for each month according to the average CF. So far, regional representative CF series of onshore wind,

TABLE 2. Installed cost per unit of different interconnector types.

HVDC Type	Line $/(MW · km)	Converter pair $/(kW)	Transmission loss	
			Line (1000km)	Converter pair
±800 overhead	99	228	2.79%	1.4%
±1100 overhead	142	202	1.60%	1.4%
±800 subsea cable	875	228	1.60%	1.4%

offshore wind, and solar PV are obtained for each month. The regional average CF during seven years and representative one year are summarized in Table 1.

B. HOURLY HYDRO POWER SERIES

It is much more difficult to precisely simulate the hourly hydro generation which is related to the instant inflow into hydro dams together with the cascading effects among dams along the same river, but hydro dams play an important role in providing flexibility to the grid.

Monthly CF, characterizing the seasonal effects of the hydro generation, is utilized in this study. Specifically, hydro power will be dispatched with hourly available quantity subject to monthly capacity factor. This is reasonable because hydro power is less fluctuating and intermittent, and most hydro dams are equipped with reservoirs.

However, monthly CF cannot be directly obtained for most countries globally, so multi-year monthly hydro generation from International Energy Agency (IEA) [48] and annual hydro CF in 2019 from International Hydropower Association (IHA) [49] are combined to generate the hydro power series of each country. The monthly generation series from IEA is normalized for each year and one representative piece is selected using previous DBSCAN clustering algorithm, and multiplied with annual CF from IHA, the monthly CF is finally obtained.

The regional equivalent monthly CF series is aggregated from sub-regional ones (countries), taking hydro potential from World Energy Council (WEC) [50] as the weight. Regional CF of hydro generation is shown in Table 1.

C. HOURLY DEMAND TIME SERIES

Besides those of most countries in Europe, hourly full year electricity demand series of 15 countries are collected from official websites or personal collaboration, e.g., the US, Brazil, Australia, Russia, South Africa, Iran, Qatar and Malaysia.

For another 13 countries, typical one-day demand series and monthly demand can be collected instead of full year series, in which case, a similar method proposed in [35] and [36] is employed to generate multi-year demand series where Gaussian noise and spline interpolation are utilized. At least two typical days can be obtained for most countries, e.g., Saudi Arabia (summer and winter), Nigeria (wet and dry season), Morocco (4 seasons), India, Thailand, and Mozambique (12 months).

The demand series for major countries within each region has been collected and those of remaining countries are simply assumed to be similar with its neighbours due to the heavy data paucity, such as North Korea, Myanmar, and countries in central Asia.

Based on the gathered demand series and projected electricity consumption in 2050, regional demand series are finally derived following the previous method.

All the data sources of historical hydro generation and demand series are summarized in Table A-I.

D. DISTANCE, TRANSMISSION LOSS AND COSTS

In this study, the geographic centre (centroid) of each region is treated as the equivalent super electricity node, which is calculated as follows.

$$\begin{cases} X = \dfrac{\sum_{i=1}^{N} x_i}{N} \\ Y = \dfrac{\sum_{i=1}^{N} y_i}{N} \end{cases} \tag{5}$$

where, X and Y represent the longitude and latitude of the centroid and (x_i, y_i) are points on the boundary of a region and a total of N points form the geometry shapes of the region. For region of 'Asia_SE' composed of several islands, it is expected to be less economical to connect them all, so some are excluded and hence the geographic center locates in Malay Peninsula.

Regarding the distance between two points on the Earth, a Python package called 'pyproj' offering interfaces to PROJ.4 is utilized where the forward and back azimuths, plus distances between initial and terminus point will be returned under the setting of 'ellps=WGS84'.

It is noted that the distance ignores the regional internal transmission grid and if considered, the distance will be shorter. Thus, the distance figures in use will penalize the use of interconnectors between the 14 regions, and hence result in conservative planning decisions of interconnectors.

Three types of HVDC interconnector are employed to interconnect regions, namely, ±800 overhead line, ±800 subsea cable both with rated 8 GW and ±1100 overhead line with 12 GW. The installed costs of transmission line and converter stations are shown in Table 2 [12], [13]. The route/interconnector sequence number (NO.), types, distance and investment costs together with transmission loss for 20 interconnectors between 14 regions are summarized in Table 3. A ±800 overhead line has the economic transmission distance of 2400 km [21] and is selected for interconnectors with distance around 2400 km or shorter in this study, shown in Fig. 1.

TABLE 3. Installed costs and transmission loss of interconnectors.

Route NO.	Region 1	Region 2	HVDC	Distance (km)		Installed costs ($/kW)/single line				Overall Loss (%)
				Land	Sea	Land	Sea	Converter pair	Sum	
1	EU_Plus	RU_WestPlus	±800	2,520	0	250	0	228	478	8.43
2	RU_WestPlus	RU_East	±1100	3,470	0	494	0	202	696	6.95
3	RU_WestPlus	Asia_C	±800	1,880	0	187	0	228	415	6.65
4	RU_East	Asia_E	±1100	2,812	0	400	0	202	602	5.90
5	Asia_C	Asia_E	±1100	3,303	0	470	0	202	672	6.68
6	Asia_C	Asia_S	±800	2,463	0	244	0	228	473	8.27
7	Asia_S	Asia_E	±1100	2,995	0	427	0	202	628	6.19
8	Middle_East	EU_Plus	±1100	3,043	0	433	0	202	635	6.27
9	Middle_East	Asia_S	±1100	4,873	0	694	0	202	896	9.20
10	Middle_East	Sub_Saharan	±1100	3,187	0	454	0	202	656	6.50
11	Asia_E	Asia_SE	±1100	3,521	0	501	0	202	703	7.03
12	Asia_SE	Oceania	(±800)	3,130	2,118	311	1,853	228	2,392	13.52
13	EU_Plus	N_America_NE	(±800)	2,313	3,356	230	2,937	228	3,394	13.22
14	N_America_NE	N_America_E	±800	2,173	0	216	0	228	444	7.46
15	N_America_E	N_America_W	±1100	1,895	0	270	0	202	471	4.43
16	N_America_W	RU_East	±1100	7,070	0	1,007	0	202	1,208	12.71
17	N_America_E	S_America	±1100	6,882	0	980	0	202	1,182	12.41
18	Asia_C	Middle_East	±1100	3,736	0	532	0	202	734	7.38
19	Middle_East	RU_WestPlus	±1100	3,761	0	536	0	202	737	7.42
20	Asia_S	Asia_SE	±1100	3,444	0	490	0	202	692	6.91

Note: 1) A complete HVDC line includes the transmission line and two converter stations. 2) The interconnector of NO. 12 and NO. 13 consists both types of ±800 overhead and ±800 subsea cable (three segments).

E. KEY PARAMETERS AND FINANCIAL ASSUMPTIONS

Table A-II shows a) regional maximum potential of solar PV, onshore and offshore wind generation calculated using method in Part A; b) regional expected RE installed capacities in 2030 collected from a series of RE roadmaps ('REmap 2030') released by International Renewable Energy Agency as well as national RE development plan, and c) regional projected demands in 2050 [4]. Table A-III summarise the financial assumptions and key parameters of solar PV and Li-ion batteries [51], hydropower [52] and wind infrastructure [53]. It should be emphasized that herein the relatively lower projected cost data are used for Solar and Energy Storage, compared to [54]–[56] while the cost data used for UHVDC are taken from recent projects and assumed to be unchanged in the future. Such assumptions for cost data would encourage more local installations of solar and energy storage rather than transmission interconnectors, which will lead to conservative results for interconnections, i.e., lower interconnection capacities.

III. MATHEMATICAL MODELS

A. MODELLING OF RE GENERATION SOURCES, STORAGE SYSTEMS, AND INTERCONNECTORS

For a 100% RE-based electricity system, it is necessary for RE sources to join the system dispatch.

$$p^{RE}_{t,i,j,z} \le P^{avi}_{t,i,j,z} \tag{6}$$

where $p^{RE}_{t,i,j,z}$, $P^{avi}_{t,i,j,z}$ denotes the dispatched and available power at time t from RE type i during the representative week of month j in region z, respectively.

The electricity storage systems also play a vital role in balancing the system, which are modelled as (6).

$$\begin{cases} E_{t,j,z} = (1-\tau)E_{t-1,j,z} + (p^{ch}_{t,j,z}\eta_{ch} - p^{dis}_{t,j,z}/\eta_{dis})\Delta t \\ E_{0,j,z} = E_{T,j,z} \\ \gamma^{min}\psi^{st}_{z} \le E_{t,j,z} \le \gamma^{max}\psi^{st}_{z} \end{cases} \tag{7}$$

where $p^{ch}_{t,j,z}$ and $p^{dis}_{t,j,z}$ are the charging and discharging powers of the storage at time t in region z. η_{ch} and η_{dis} are the charging and discharging efficiency. Δt denotes the time interval. $E_{t,j,z}$, $E_{t-1,j,z}$, $E_{0,j,z}$, and $E_{T,j,z}$ denote the electricity stored at times t, t-1, 0, and T, and ψ^{st}_{z} is the installed capacity. γ^{min} and γ^{max} [0.1 and 0.9 in this study] are the minimum and maximum SoC requirements and the system cycles at 80% Depth of Discharge.

A complete HVDC link normally comprises of one transmission line and two converter stations. It is modelled as (7), where the power loss through transmission line and converter stations are included.

$$p^{end}_{t,j,z,n} = p^{start}_{t,j,z,n}\left[1 - \left(\delta^{li}L_{z,n} + \delta^{te}\right)\right] \tag{8}$$

where $p^{start}_{t,j,z,n}$ and $p^{end}_{t,j,z,n}$ are the powers at the starting and ending points of the interconnector at time t with the power transferring from region z to region n. $L_{z,n}$ and δ^{li} are the distance between region z and region n, and the corresponding transmission loss. δ^{te} is the power conversion loss in converter stations.

B. PLANNING MODEL COUPLED WITH DISPATCH

A planning optimization model coupled with economic dispatch to determine the regional additional capacities of RE

TABLE 4. Case specifications.

Case	Solar	Wind	Hydro	Energy Storage	Load Curtailment	Interconnection
1	Y	N	N	Y	Y, 5%	N
2	N	Y	N	Y	Y, 5%	N
3	Y	Y	N	Y	Y, 5%	N
4	**Y**	**Y**	**Y**	**Y**	**Y, 5%**	**N**
5	Y	N	N	Y	Y, 5%	Y
6	N	Y	N	Y	Y, 5%	Y
7	Y	Y	N	Y	Y, 5%	Y
8	Y	Y	Y	Y	Y, 5%	Y
9	Y	N	N	N	Y, 5%	Y
10	N	Y	N	N	Y, 5%	Y
11	Y	Y	N	N	Y, 5%	Y
12	Y	Y	Y	N	Y, 5%	Y
13	Y	N	N	Y	N	N
14	N	Y	N	Y	N	N
15	Y	Y	N	Y	N	N
16	Y	Y	Y	Y	N	N
17	Y	N	N	Y	N	Y
18	N	Y	N	Y	N	Y
19	Y	Y	N	Y	N	Y
20	Y	Y	Y	Y	N	Y
21	Y	N	N	N	N	Y
22	N	Y	N	N	N	Y
23	Y	Y	N	N	N	Y
24	Y	Y	Y	N	N	Y

Note: For a technology not considered, e.g., 'Hydro' in Case 1, the existing capacity in 2030 is dispatched to supply the grid.

sources, storage systems as well as the interconnectors among regions was presented. The incorporated dispatch was run for 12 months at hourly resolution. The base year and target year are 2030 and 2050, respectively. The total investment in all additional infrastructures since 2030 is calculated based on the electricity demands of 2050. It is also assumed that there would be no existing interconnections and large-scale storage systems by 2030. The optimization model is coded in Matlab 2019a coupled with Yalmip and Gurobi 8.1.1, and run on the same laptop as the data processing in Section II.

1) OBJECTIVES AND CONSTRAINTS

The total cost, expressed as annual cost, consist of a) the annualized overnight capital costs, b) fixed operation and maintenance (O&M) costs and c) variable O&M costs. The objective function is as follows.

$$min \left\{ \begin{array}{l} [\sum_{i,z}(CRF_i \psi_{i,z} \omega_{i,z} + \emptyset_i^{\text{fix}} \psi_{i,z} \omega_{i,z}) + \sum_{t,i,z} \emptyset_i^{\text{var}} p_{t,i,z}] \\ + \left[\sum_{I \in \Omega}(CRF_I(\psi_I + \mathrm{C})\omega_I + \emptyset_I^{\text{fix}} \psi_I \omega_I)\right] \end{array} \right\} \tag{9}$$

where CFR_i is the capital recovery factors (CFR) of different RE technologies, energy storage systems and interconnectors, calculated using (9). $\psi_{i,z}$ and $\omega_{i,z}$ are the installed capacity and capital cost per unit of technologies in region z. $\emptyset_i^{\text{fix}}$ and $\emptyset_i^{\text{var}}$ are the fixed and variable operational and maintenance expenditure of technology i. $p_{t,i,z}$ is the power output of technology i in region z at time t. $\sum_{I \in \Omega}(CRF_I(\psi_I + C)\omega_I + \emptyset_I^{\text{fix}} \psi_I \omega_I)$ are the interconnector related costs where I denotes an interconnector between a certain pair of regions, Ω is a set including all interconnection routes, and C is a constant, denoting the rated capacity of a single DC line, which is related to 'N-1' security criterion and explained in next section.

TABLE 5. Interconnector capacity and cost.

Route NO.	Capacity (GW)	Annual cost (billion $)		
		Capital	O&M	*Sum*
1	409	14.0	2.9	*17*
2	138	6.8	1.3	*8*
3	169	5.0	1.0	*6*
4	564	24.4	5.0	*29*
5	218	10.4	2.1	*12*
6	151	5.0	1.0	*6*
7	74	3.2	0.6	*4*
8	94	4.2	0.8	*5*
9	84	5.3	1.0	*6*
10	46	2.0	0.3	*2*
11	18	0.8	0.1	*1*
12	24	4.1	0.6	*5*
13	0	0.0	0.0	*0*
14	245	7.8	1.6	*9*
15	412	13.9	2.8	*17*
16	545	47.5	9.7	*57*
17	136	11.5	2.2	*14*
18	62	3.1	0.6	*4*
19	0	0.0	0.0	*0*
20	179	8.8	1.7	*11*
Sum	*3,568*	*178*	*35*	*213*

$$CRF_i = \frac{WACC(1+WACC)^y}{(1+WACC)^y - 1} \tag{10}$$

where a weighted average cost of capital (WACC) of 7% is set to all technologies and y is technology's lifetime.

The constraints of the planning model include a) installed capacity limits of facilities, b) hourly power balance of the whole system, c) hourly power output limits of infrastructure.

2) N-1 SECURITY CRITERION

It is worth noting that the 'N-1' criterion for global electricity interconnection in this study is much stricter than the traditional definition. The traditional 'N-1' security means that if a component – e.g. a transformer or circuit – should fail or be shut down in a network operating at the maximum forecast levels of transmission and supply, the network security must still be guaranteed. In contrast, for the 'N-1' criterion in this study, it allows outage of any single line from each interconnection route, which consists of multiple transmission lines. Specifically, this means for global electricity interconnection

TABLE 6. Overall additional and exsting capacity (GW).

Region	Without interconnection					With interconnection				
	Onshore	Offshore	Solar	Hydro	Storage	Onshore	Offshore	Solar	Hydro	Storage
EU_Plus	1,438	124	1,186	334	1,717	255	72	739	139	511
RU_WestPlus	296	0	19	167	478	1,251	0	11	28	0
RU_East	88	0	29	46	92	576	0	0	46	216
Middle_East	280	0	1,763	53	5,859	529	0	1,389	53	3,018
Asia_C	46	0	180	16	402	585	0	6	16	12
Asia_S	188	3	4,091	204	12,786	188	3	3,004	92	9,441
Asia_E	711	52	10,260	475	24,404	966	52	6,667	475	10,254
Asia_SE	15	0	2,553	103	6,592	15	0	2,247	103	5,310
Oceania	50	0	103	34	339	88	0	56	13	86
Sub_Saharan	31	0	1,270	93	4,183	220	0	950	93	2,793
N_America_W	130	4	422	142	911	130	1	1,222	90	398
N_America_E	771	41	2,734	124	6,584	267	41	1,586	72	2,193
N_America_NE	31	2	112	68	165	452	2	3	62	0
S_America	44	0	1,016	183	2,923	44	0	784	183	1,197
Sum	4,118	227	25,739	2,042	67,435	5,568	172	18,663	1,465	35,431

Note: The capacity of storage system is expressed as GWh

TABLE 7. Regional additional annual cost and its breakdowns (Billion $).

Region	Without interconnection							With interconnection						
	On-shore	Off-shore	Solar	Hydro	Storage	Load Curtailment	*Sum*	On-shore	Off-shore	Solar	Hydro	Storage	Load Curtailment	*Sum*
EU_Plus	117.8	13.4	22.9	30.1	22.0	4.2	210	0.0	0.0	11.7	0.4	6.6	0.5	19
RU_WestPlus	28.3	0.0	0.2	22.2	6.1	0.7	58	123.3	0.0	0.0	0.0	0.0	0.0	123
RU_East	8.5	0.0	0.7	0.2	1.2	0.2	11	57.1	0.0	0.0	0.1	2.8	0.0	60
Middle_East	19.9	0.0	40.6	0.0	75.6	2.0	138	44.8	0.0	31.2	0.1	39.0	0.4	116
Asia_C	3.7	0.0	4.4	0.0	5.2	0.3	14	57.5	0.0	0.0	0.0	0.2	0.0	58
Asia_S	0.0	0.0	97.4	17.7	165.4	5.3	286	0.0	0.0	70.2	0.6	122.1	0.3	193
Asia_E	25.6	0.0	244.5	0.5	315.4	18.7	605	51.0	0.0	154.6	2.2	132.6	0.0	340
Asia_SE	0.0	0.0	62.4	0.3	85.3	0.4	148	0.0	0.0	54.7	0.6	68.7	0.1	124
Oceania	3.0	0.0	1.7	3.4	4.4	0.2	13	6.9	0.0	0.5	0.0	1.1	0.1	9
Sub_Saharan	0.0	0.0	31.2	0.5	54.1	0.6	86	18.9	0.0	23.2	0.5	36.1	0.1	79
N_America_W	0.0	0.7	9.2	8.9	11.8	0.8	31	0.0	0.0	29.2	0.3	5.1	0.0	35
N_America_E	54.5	0.0	65.6	8.1	84.8	3.8	217	4.4	0.0	36.9	0.3	28.3	0.0	70
N_America_NE	2.1	0.0	2.7	1.9	2.1	0.6	9	44.1	0.0	0.0	0.2	0.0	0.0	44
S_America	0.0	0.0	25.0	2.2	37.8	1.2	66	0.0	0.0	19.2	1.9	15.5	0.0	37
Sum	*264*	*14*	*608*	*96*	*871*	*39*	*1,892*	*408*	*0*	*431*	*7*	*458*	*1*	*1,306*

Note: The cost sum of all technologies in the last column, i.e., 1306 billion $ excludes the cost of transmission links (213 billion $).

that if there are K interconnection routes, it allows that K transmission lines (one transmission line for each route) can be disconnected simultaneously any time under all the operating conditions. In order to meet the 'N-1' criterion and guarantee the supply reliability, this is implemented in the system model by adding an additional DC line into the interconnector between two regions, i.e., constant C in the objective function. The rated capacity of a single DC line of ±800 and ±1100 kV transmission is 8 GW and 12 GW respectively.

IV. RESULTS

A. CASE SPECIFICATIONS

A total of 24 cases are comprehensively compared in this study, shown in Table 4 where 'Y' in the column of a technology indicates that this particular type of technology is selected and additional capacity is optimally proposed from 2030. Hence, the overall existing capacity in 2030 and additional capacity since 2030 can be dispatched but for technologies not selected ('N'), only exiting capacity in 2030 can be dispatched.

TABLE 8. Overall capacity (GW) and annual cost (Billion $) globally.

Case	Capacity					Annual Cost									
	On shore	Off-shore	Solar	Hydro	Storage	Load Curtail	On-shore	Off-shore	Solar	Hydro	Storage	Link	*Sum*	Drop (%)*	Extra (%)*
1	1,471	172	41,415	1,465	85,866	33	0	0	1,001	5	1,109	0	*2,148*	-13.5	0.0
2	-	-	-	-	-	-	-	-	-	-	-	-	-	-	0.0
3	4,640	267	26,849	1,465	68,999	41	316	25	636	5	891	0	*1,914*	-1.1	0.0
4	**4,118**	**227**	**25,739**	**2,042**	**67,435**	**39**	**264**	**14**	**608**	**96**	**871**	**0**	***1,892***	**Ref.**	**0.0**
5	1,471	172	28,152	1,465	61,256	10	0	0	669	5	792	209	*1,686*	10.9	0.5
6	17,760	172	1,413	1,465	9,285	50	1,622	0	0	4	119	372	*2,166*	-14.5	0.4
7	5,568	172	18,663	1,465	35,431	1	408	0	431	7	458	213	*1,519*	19.7	0.5
8	5,568	172	18,663	1,465	35,431	1	408	0	431	7	458	213	*1,519*	19.7	0.5
9	1,471	172	56,281	1,465	0	26	0	0	1,372	3	0	1,681	*3,083*	-62.9	0.3
10	21,671	172	1,413	1,465	0	18	2,011	0	0	1	0	382	*2,413*	-27.5	0.3
11	13,080	172	11,741	1,465	0	24	1,156	0	258	2	0	399	*1,839*	2.8	0.5
12	11,752	172	10,268	2,612	0	26	1,024	0	221	185	0	354	*1,811*	4.3	0.4
13	1,471	172	43,010	1,465	89,517	0	0	0	1,040	4	1,156	0	*2,200*	-16.3	0.0
14	-	-	-	-	-	-	-	-	-	-	-	-	-	-	0.0
15	4,354	238	29,035	1,465	73,941	0	287	17	691	4	955	0	*1,954*	-3.3	0.0
16	3,848	210	27,073	2,192	71,422	0	237	10	642	119	922	0	*1,930*	-2.0	0.0
17	1,471	172	28,614	1,465	60,367	0	0	0	680	4	781	230	*1,695*	10.4	0.5
18	18,651	172	1,413	1,465	12,052	0	1,711	0	0	3	155	346	*2,214*	-17.0	0.4
19	5,502	172	18,732	1,465	35,960	0	401	0	433	7	465	213	*1,520*	19.7	0.5
20	5,502	172	18,732	1,465	35,959	0	401	0	433	7	465	213	*1,520*	19.7	0.5
21	1,471	172	57,115	1,465	0	0	0	0	1,393	2	0	1,859	*3,254*	-72.0	0.3
22	23,157	172	1,413	1,465	0	0	2,159	0	0	0	0	404	*2,564*	-35.5	0.3
23	13,819	172	13,033	1,465	0	0	1,229	0	291	1	0	406	*1,927*	-1.8	0.5
24	12,420	172	11,516	2,617	0	0	1,090	0	253	182	0	361	*1,885*	0.4	0.4

Note: 1) '-' in Table VIII indicates that the solution is infeasible. 2) 'Drop (%)' shows the annual cost drop of all the cases w.r.t Reference Base Case 4. 3) 'Extra (%)' is the percentage of sum of extra interconnector costs (an additional DC line) considering '*N*-1' security criterion over the total annual cost.

- The difference between the set of Case 1 $\sim$ 12 and the set of Case 13 $\sim$ 24 is whether to consider load curtailment in the planning model. First 12 cases consider a load curtailment of 5% of the total regional load, meaning that 5% the demand is allowed to be curtailed when dispatched via market balancing services in the range of around 100 $\sim$ 20,000 £/MWh [57], and in this study 2000 £/MWh (equivalent to 2600 $/MWh) is used. In contrast, the remaining 12 cases do not consider the load curtailment. Meanwhile, Case 4 is taken as the base reference case in this study.
- The difference between first set of cases (i.e., Case 1 $\sim$ 4) and second set of four cases (i.e., Case 5 $\sim$ 8) is whether to consider interconnection between regions in the planning model. It is worth noting that the actual interconnection schemes are determined by the decisions of the optimal planning model.
- The difference between the third set of four cases (i.e., Case 9 $\sim$ 12) and the second set of four cases (i.e., Case 5 $\sim$ 8) is whether energy storage is considered.

B. PLANNING RESULTS OF OPTIMAL CASE – CASE 8

Proposed capacities along with costs of interconnectors and regional RE installations of the 100% RE system are shown in Table 5 and Table 6. Regional additional annual cost and its breakdowns are summarized in Table 7.

It is shown in Table 5 and Table 7 that the annual cost of the whole system will fall from 1892 billion USD ($) of the Base Reference Case (Case 4) to 1519 billion USD of the optimal case (i.e., Case 8), approximately 19.7% with the interconnection being considered, and the interconnectors accounting for 14.0% of the overall cost. This is directly led by the capacity reductions of solar PV, hydro, and storage systems. There are primarily two reasons behind the reductions: 1) grid interconnection makes less need of regional generating capacities to deal with the short-term variability of net-load (difference between load and supply); 2) the RE sources are deployed optimally in a wider geographical scale and thus regions with higher CF are proposed to install more capacities, and hence greatly decreasing overall installations, e.g., 'RU_WestPlus', 'Asia_C', and 'N_America_NE' with higher onshore wind power CF will install much more onshore wind generation sources while 'N_America_W' with higher solar power CF will install more solar PV.

When the interconnections exist, the additional capacities of hydro and offshore wind resources are not proposed in any regions though they generally have higher CF than the other generation resources. This is because their capital

TABLE 9. Interconnector capacity (GW).

Route NO.	Cases with load curtailment 5%								Cases without load curtailment 0%							
	5	6	7	8	9	10	11	12	17	18	19	20	21	22	23	24
1	53	246	409	409	396	344	505	472	70	197	401	401	493	481	510	512
2	57	247	138	138	1,476	48	415	283	136	221	147	147	1,631	27	433	334
3	1	245	169	169	0	151	382	430	1	107	165	165	1	222	331	432
4	533	891	564	564	2,365	1,002	888	890	527	1,341	557	557	2,344	979	836	872
5	48	750	218	218	37	440	591	488	30	582	232	232	38	459	584	517
6	2	56	151	151	0	348	573	563	28	99	143	143	1	325	582	561
7	230	194	74	74	0	163	133	167	169	153	71	71	0	155	132	153
8	449	262	94	94	185	144	83	98	460	306	96	96	101	129	86	84
9	287	662	84	84	1,314	286	613	490	222	493	72	72	1,129	303	677	503
10	32	90	46	46	313	185	152	151	29	87	42	42	319	166	133	140
11	0	84	18	18	3,043	219	71	59	0	149	20	20	3,312	225	72	130
12	17	174	24	24	776	337	39	40	17	115	24	24	1,154	334	42	42
13	0	0	0	0	32	0	0	0	0	0	0	0	26	0	23	1
14	42	572	245	245	25	202	248	349	42	472	262	262	32	218	152	215
15	380	355	412	412	3,192	388	497	440	475	359	411	411	3,557	424	504	455
16	521	371	545	545	4,395	509	608	514	588	402	547	547	4,545	552	658	559
17	116	104	136	136	1,723	422	166	146	174	107	143	143	2,294	495	160	151
18	75	52	62	62	65	91	285	185	40	39	58	58	68	125	264	142
19	178	290	0	0	1,361	0	26	0	246	204	0	0	1,441	0	0	0
20	189	277	179	179	1,592	174	437	357	259	200	174	174	1,510	190	450	340

TABLE 10. Annual cost for cases with and without interconnection (Billion $).

Portfolio	Load Curtailment 5%			Load Curtailment 0%		
	Interconnection		Drop (%) / $\frac{T_N - T_Y}{T_N}$	Interconnection		Drop (%) / $\frac{T_N - T_Y}{T_N}$
	No / T_N	Yes / T_Y		No	Yes	
PV+Storage	2,148	1,686	21.5	2,200	1,695	23.0
Wind+Storage	-	2,166	-	-	2,214	-
PV+Wind+Storage	1,914	1,519	20.6	1,954	1,520	22.2
PV+Wind+Hydro+Storage	1,892	1,519	19.7	1,930	1,520	21.3

TABLE 11. Annual cost for cases under load curtailment 5% and 0% (Billion $).

Portfolio	Without interconnection			With interconnection		
	Load Curtailment		Drop (%) / $\frac{T_5 - T_0}{T_5}$	Load Curtailment		Drop (%) / $\frac{T_5 - T_0}{T_5}$
	5% / T_5	0% / T_0		0% / T_0	5% / T_5	
PV+Storage	2,148	2,200	-2.5	1,686	1,695	-0.6
Wind+Storage	-	-	-	2,166	2,214	-2.2
PV+Wind+Storage	1,914	1,954	-2.1	1,519	1,520	0.0
PV+Wind+Hydro+Storage	1,892	1,930	-2.0	1,519	1,520	0.0

expenditures are more expensive and there are also variable operation and maintenance (O&M) costs for hydro generation, which makes them less competitive compared to solar and onshore wind generation.

For the optimal case (Case 8) with interconnectors, the total capacity of energy storage is around 50% less than that of the reference case (Case 4) without interconnectors (35,431 vs 67,435 TWh), and this indicates that global electricity grid with interconnectors can bring equivalent energy storage capacity by exploring the complementary characteristics of renewable energy sources in particular solar energy with time differences. This also implies that global interconnected electricity grid can bring significant flexibility, and thus the load curtailment would become less important.

TABLE 12. Annual cost for cases with storage and with interconnection (Billion $).

Portfolio	Load Curtailment 5%			Load Curtailment 0%		
	Storage $/T_s$	Interconnection $/T_i$	Drop (%) $/\frac{T_s-T_i}{T_s}$	Storage $/T_s$	Interconnection $/T_i$	Drop (%) $/\frac{T_s-T_i}{T_s}$
PV	2,148	3,083	-43.5	2,200	3,254	-47.9
Wind	-	2,413	-	-	2,564	-
PV+Wind	1,914	1,839	3.9	1,954	1,927	1.4
PV+Wind+Hydro	1,892	1,811	4.3	1,930	1,885	2.3

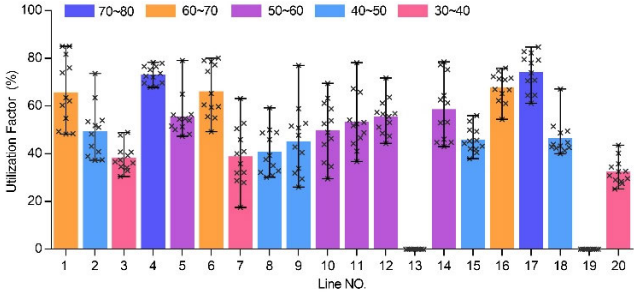

FIGURE 2. Utilization factor of interconnectors.

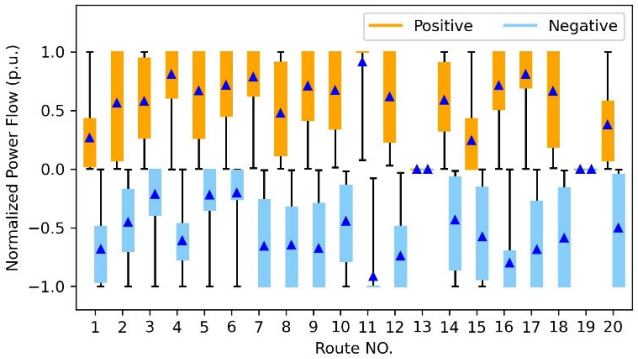

FIGURE 3. Power Flow Patterns of Interconnectors.

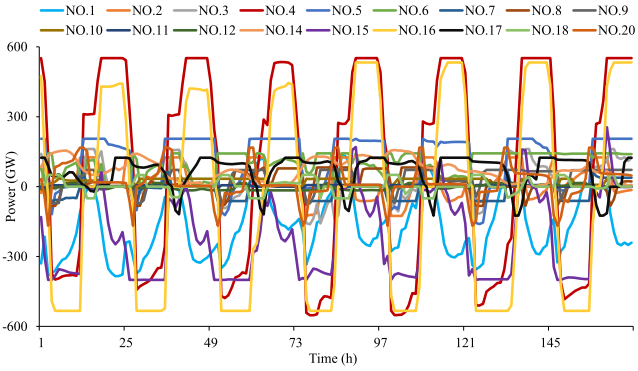

FIGURE 4. Actual Power Flows of Interconnectors.

It is shown in Table 5 that nearly 550 GW of interconnectors (Line NO. 16 and NO. 4) are proposed to connect 'N_America_W' and 'RU_East' (further reaching 'Asia_E') while 'N_America_NE' and 'EU_Plus' (NO. 13) are not recommended to interconnect because the investment cost per kW of latter route is much higher than the former due to expensive long distance submarine cable (shown in Table 3). Also, there is about a 12-hour time difference between 'N_America_E' and 'Asia_E' and 6-hour time difference between 'N_America_E' and 'EU_Plus', so the former pair of load centers has a stronger complementarity than latter pair in terms of temporal solar power availability.

From a perspective of lowering global annual cost, 'EU_Plus' and 'RU_WestPlus' (NO. 1) are recommended to interconnect using a link of 409 GW because onshore wind generation in 'RU_WestPlus' has higher CF. 'N_America_E' is recommended to connect with 'N_America_W' via a 412 GW link (NO. 15) to utilize the solar PV power there and further to interact with north-eastern part of Asia. It is also proposed for 'Asia_E' to connect with 'Asia_C' through a 218 GW interconnector (NO. 5).

The utilization factors of lines/interconnectors are shown in Fig.2, where bar values represent the annual utilization factor (UF), bar whiskers give the minimum-maximum ranges across the monthly UFs and 'x' represents the monthly UF of each interconnector. It can be found that all the deployed interconnectors have a higher annual UF than 30% where annual UFs of 15 interconnectors and 5 interconnectors are higher than 40% and 60%, respectively.

The power flow patterns of these interconnectors are shown in Fig 3 where the box spans the first to the third quartile (25 $\sim$ 75 percentile), the whiskers give the minimum-maximum ranges, and the blue triangle represents the 'mean' of the normalized power flows. From 'Region 1' to 'Region 2' is defined as the positive direction of power flows through an interconnector/route as in Table 3. The actual power flows in one week of July are shown in Fig.4.

It is worth noting in Fig. 3 that the '75 percentile' can overlap with the 'maximum' (e.g., line NO. 7), meaning the power values higher than '75 percentile' are maintained at the 'maximum'; the '25 percentile' can overlap with the 'minimum' (e.g., 'Negative' of line NO. 3) and it can also overlap with the 'maximum' (e.g., line NO.11).

As shown in Fig.3 and Fig.4, it can be found that the power flows of the interconnectors are changing dynamically over a wide range during a week, which indicates the value of interconnectors to facilitate the complementarity of diversified energy sources in different geographical regions and

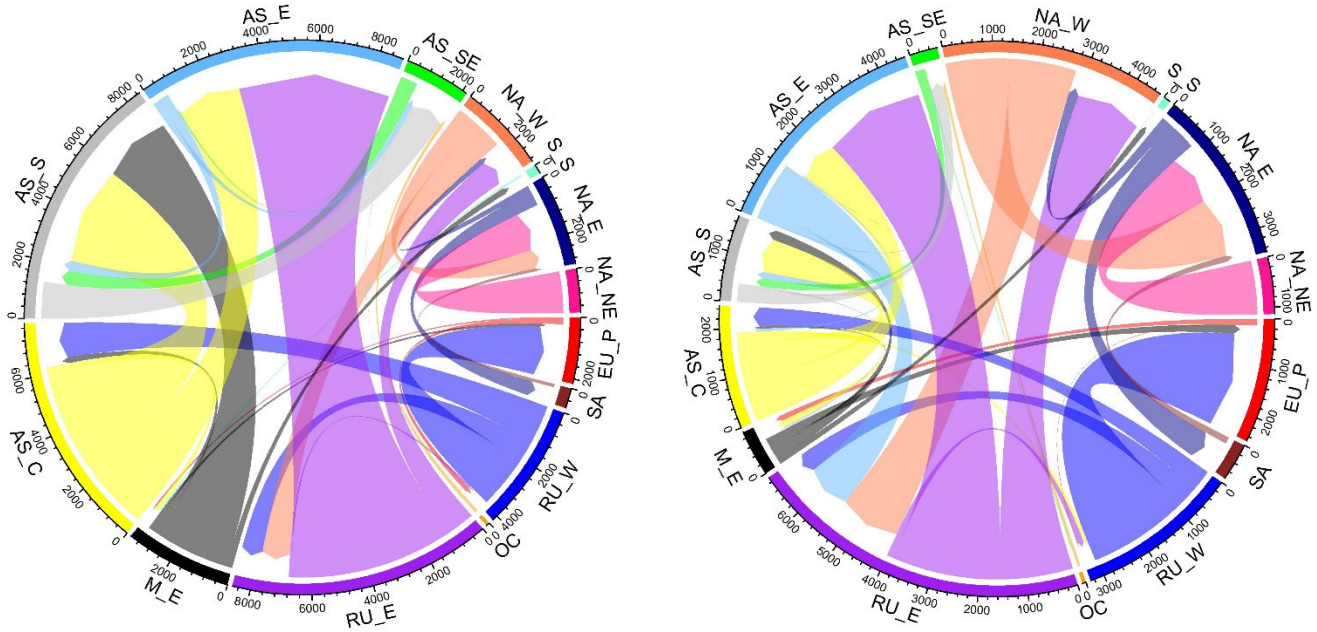

(a) Case 12: PV+Wind+Hydro

(b) Case 8: PV+Wind+Hydro+Storage

FIGURE 5. Annual electricity flow through interconnectors for Case 8 and Case 12.

bring their market value into the real time balancing between demand and generation.

C. PLANNING RESULTS OF ALL CASES

The proposed global capacities and annual cost of solar PV, onshore wind, offshore wind, hydro and energy storage together with interconnectors between regions for all 24 cases are summarized in Table 8 and Table 9.

As in Table 8, there are no feasible results for Case 2 and Case 14 that rely on wind generation and energy storage to supply the regional demand without the consideration of interconnection. The reason is that regional demand in 'Asia_S' cannot be met by local wind generation only even under the assumption that extremely high capacity of energy storage is allowed. Specifically, calculated based on the maximum capacity of onshore and offshore wind power for 'Asia_S' (Table A-III) and corresponding CF (Table 1), the annual wind power production in 'Asia_S' is 3962 TWh while its annual demand (Table A-III) is 6,660 TWh (much higher than regional annul wind production), which leads to the infeasibility of optimization model.

1) N-1 SECURITY CRITERION

As in the last column of Table 8, the extra interconnector costs for considering 'N-1' security criterion (an additional DC line) take up less than 1% of the overall annual cost in all cases. In other word, 'N-1' security consideration of the interconnectors between 14 regions has just made a small contribution of less than 1% to the total annual costs.

Take Case 8 as an example, the sum of an additional DC line for all interconnection routes, except for route NO. 13 and NO 19 whose capacity is 0 in optimal decisions shown in Table 5, is 7.99 billion $ and it accounts for approximately 0.53% of the annual cost (1519 billion $) of Case 8.

2) WITH VS WITHOUT INTERCONNECTION

The annual costs for cases with and without interconnection are respectively shown in Table 10 and Table 11 corresponding Case 1 $\sim$ Case 8 and Case 13 $\sim$ Case 20.

Under the same load curtailment percentage, the annual cost drop of a portfolio with the interconnection is calculated with regard to (w.r.t) the annual cost of this portfolio without the interconnection. Under the same interconnection consideration, the annual cost drop for a portfolio without load curtailment (0%) is calculated w.r.t. the annual cost of this portfolio with load curtailment (5%) and is usually a negative value, indicating that the annual cost will increase if the load curtailment is not allowed.

As in Table 10, the interconnection between regions will yield a minimum saving of 20% (19.7% exactly) of overall annual cost for all supply portfolios of 'RE sources + Storage system' under the load curtailment factor of 5% and without the load curtailment slightly increases this saving to 21%.

Regarding 'with vs without load curtailment' as in Table 11, without the load curtailment will increase the annual cost by approximately 2% for cases without the interconnection but it can hardly influence the cost for cases with the interconnection, indicating less need for load curtailing after the interconnection is considered for portfolios of 'RE sources + Storage system'.

3) STORAGE VS INTERCONNECTION

In order to compare the benefits introduced by energy storage system and the interconnection, four portfolios of generating

TABLE 13. Annual cost for cases under load curtailment 5% and 0% (Billion $).

Portfolio	With storage			With interconnection		
	Load Curtailment 5% /T_5	Load Curtailment 0% /T_0	Drop (%) /$\frac{T_5-T_0}{T_5}$	Load Curtailment 5% /T_5	Load Curtailment 0% /T_0	Drop (%) /$\frac{T_5-T_0}{T_5}$
PV	2,148	2,200	-2.5	3,083	3,254	-5.6
Wind	-	-	-	2,413	2,564	-6.3
PV+Wind	1,914	1,954	-2.1	1,839	1,927	-4.8
PV+Wind+Hydro	1,892	1,930	-2.0	1,811	1,885	-4.1

TABLE 14. Annual cost for cases with different load curtailment cost (Billion $).

Case	Solar	Wind	Hydro	Energy Storage	Interconnection	Load Curtailment (£/MWh)		Drop (%) /$\frac{T_1-T_2}{T_1}$
						2000 /T_1	20,000 /T_2	
1	Y	N	N	Y	N	2148	2,200	-2.5
2	N	Y	N	Y	N	-	-	-
3	Y	Y	N	Y	N	1914	1,954	-2.1
4	Y	Y	Y	Y	N	1892	1,930	-2.0
5	Y	N	N	Y	Y	1,686	1,695	-0.6
6	N	Y	N	Y	Y	2,166	2,215	-2.3
7	Y	Y	N	Y	Y	1,519	1,520	0.0
8	Y	Y	Y	Y	Y	1,519	1,520	0.0
9	Y	N	N	N	Y	3,083	3,163	-2.6
10	N	Y	N	N	Y	2,413	2,491	-3.3
11	Y	Y	N	N	Y	1,839	1,910	-3.8
12	Y	Y	Y	N	Y	1,811	1,875	-3.5

technologies are proposed, i.e., 'PV' only, 'Wind' only, 'PV+Wind', and 'PV+Wind+Hydro'. They are combined with either energy storage system or interconnection to supply the whole electricity system and the results are shown in Table 12 and Table 13.

It can be found in Table 12 that with a single generation technology, the annual cost is much higher than hybrid generation technologies where the complementarity among solar PV and wind power is utilized. Specifically, the combination of 'PV' and 'Interconnection' will necessitate a large amount of interconnector capacities, especially those spanning several time zones. Take Case 9 (load curtailment 5%, 'Interconnection' and 'PV') as an example, more than 3200 GW of interconnectors between 'N_America_E', 'RU_East' through 'N_America_W' is proposed where 12-hour difference and strong solar PV complementarity exists (Table 9). More than 1000 GW of interconnectors are proposed between 'RU_WestPlus' and 'RU_East', and between 'Middle_East', 'Asia_S', and 'Asia_SE'. Additionally, regions of 'Middle-East' and 'Asia_SE' that are close to the equator have higher capacity factor and annual availability of solar power and hence will act as the generation base under single 'PV' scenario, so related interconnectors are also proposed with high capacity, e.g., that between 'Middle-East' and 'RU_WestPlus' and those between 'Asia_SE', 'Asia_E' and 'RU_East'. Therefore, the annual cost for portfolio of single solar PV and interconnection is significantly higher than other portfolios (more than 3000 billion USD).

In general, when the complementarity between local renewable energy sources is exploited, e.g., 'PV+Wind+Hydro', interconnection perform slightly better than storage system with a cost decrease by 4% (4.3% exactly) under a load curtailment of 5% and by 2% (2.3% exactly) without load curtailment.

Regarding 'with vs without load curtailment', without load curtailment will increase the annual cost by at least 4% for portfolios of 'RE sources + Interconnection' while 2% for 'RE sources + Storage system', shown in Table 13.

4) COST PER UNIT OF LOAD CURTAILMENT

As introduced in section A, 5% of the demand is allowed to be curtailed in this study when dispatched via market balancing services in the range of around 100 $\sim$ 20000 £/MWh. In previous analysis, a cost of 2000 £/MWh (equivalent to 2600 $/MWh) for load curtailing is used, and in current analysis the impact that different load curtailment cost per unit have on the annual cost will be investigated. The annual costs of 12 cases with a load curtailment of 5% based on a cost of 2600 $/MWh and 26000 $/MWh respectively are shown in Table 14.

For all the cases with portfolios of 'RE sources + Storage system' (Case 1 $\sim$ 4) and 'RE sources + Interconnection'

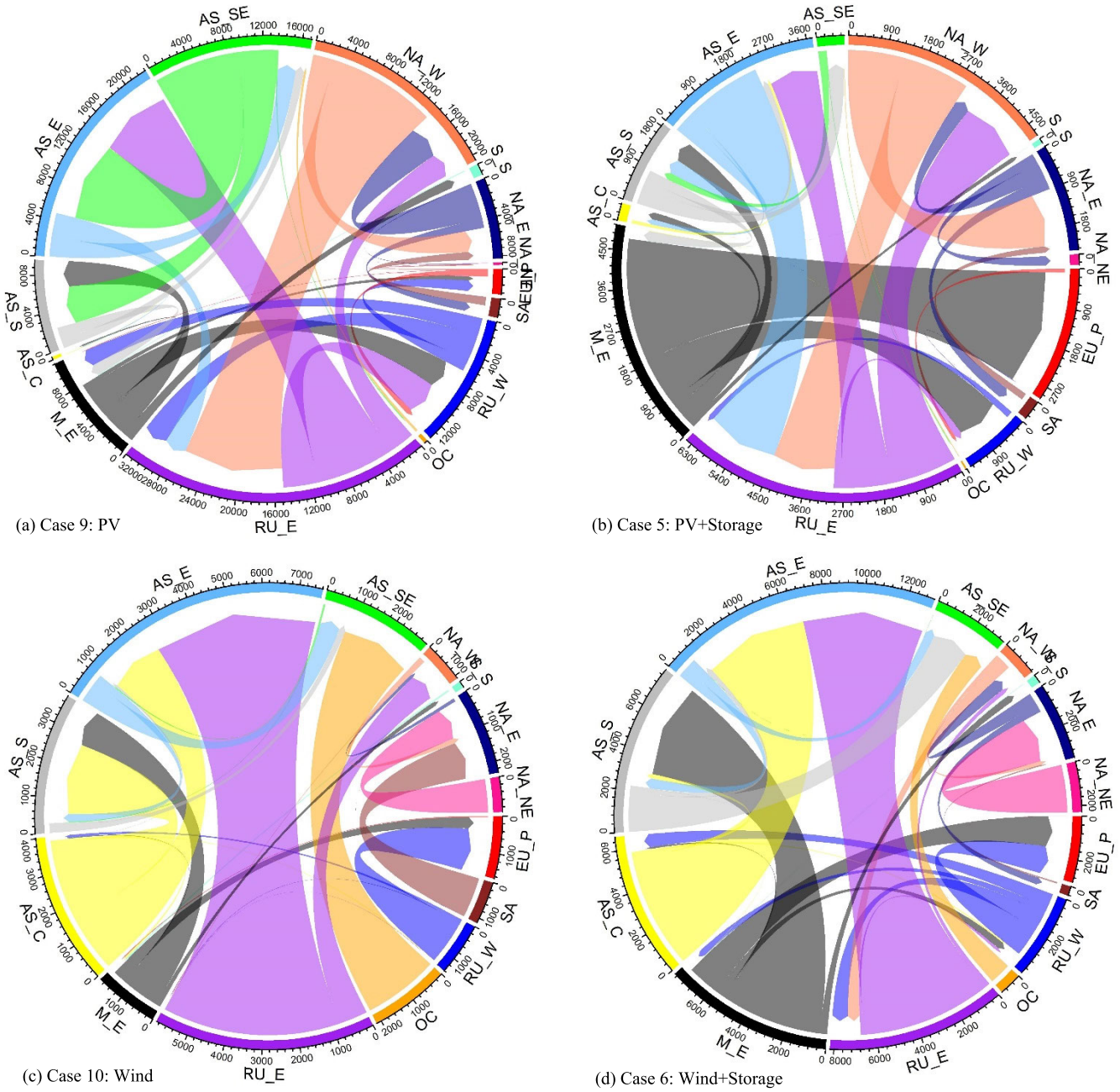

(a) Case 9: PV

(b) Case 5: PV+Storage

(c) Case 10: Wind

(d) Case 6: Wind+Storage

FIGURE 6. Annual electricity flow through interconnectors for other cases.

(Case 9 ∼ 12), high load curtailment cost of up to 10 times (2600 vs 26000 $/MWh) increases the annual cost by 2% ∼ 4%. In contrast, for cases with portfolios of 'RE sources + Storage system + Interconnection', high curtailment cost hardly increases the annual cost when both wind and solar power are considered.

D. ANNUAL ELECTRICITY ENERGY FLOW

The annual cumulative electricity energy flows (TWh) through the interconnectors for optimal case (Case 8) as well as Case 12 are illustrated respectively in Fig. 5, where a load curtailment factor of 5% is considered. It is noted that a region's name is further abbreviated for better illustration, e.g., 'E_P' for 'EU_Plus', and 'RU_E' for 'RU_East'.

As in Fig.5(b), the difference between the in-flow and out-flow is the regional annual net import of electricity. For electricity energy flow of optimal case (Case 8), 'Asia_E', 'Asia_S', 'EU_Plus' and 'N_America_E' are dominated by import due to their higher demand levels. 'Asia_C', 'RU_West' and 'N_America_NE' are dominated by the export because they have lower demand levels but are blessed

TABLE 15. Sources of historical statistics.

Row	Country	Source and Website
1	OECD	IEA: https://www.iea.org/reports/monthly-electricity-statistics
2	Europe	Eurosat: http://appsso.eurostat.ec.europa.eu/nui/show.do?dataset=nrg_105m
3	China	http://data.stats.gov.cn/easyquery.htm?cn=E0101
4	US	EIA: https://www.eia.gov/electricity/data.php#generation
5	CA	Canada: https://www150.statcan.gc.ca/t1/tbl1/en/tv.action?pid=2510001501
6	Russia	UPS: https://so-ups.ru/functioning/ees/ups-review/ups-review20/
7	Europe	ENTSO-E: https://tyndp.entsoe.eu/maps-data
8	US	EIA: https://www.eia.gov/todayinenergy/detail.php?id=27212
9	Canada	ESO: Alberta, British Columbia, New Brunswick, Ontario
10	Japan	Power companies websites: Chubu, Chugoku, Hokkaido, Hokuriku, Kansai, Kyushu, Shikoku, Tohoku, Tokyo
11	China	http://www.gov.cn/xinwen/2019-12/30/content_5465088.htm
12	Malaysia	https://www.gso.org.my/SystemData/SystemDemand.aspx
13	Singapore	https://www.ema.gov.sg/statistic.aspx?sta_sid=20140826Y84sgBebjwKV
14	Argentina	https://cammesaweb.cammesa.com/parte-semanal/
15	Australia	https://www.aemo.com.au/energy-systems/electricity/national-electricity-market-nem/data-nem/aggregated-data
16	Brazil	http://www.ons.org.br/Paginas/resultados-da-operacao/historico-da-operacao/curva_carga_horaria.aspx
17	South Africa	https://www.eskom.co.za/sites/publicdata/Pages/default.aspx
18	Chile	https://www.coordinador.cl/operacion/graficos/operacion-real/
19	Iran	https://www.igmc.ir/Documents/EntryId/305927
20	Russia	https://www.so-ups.ru/functioning/ees/ees-2020/
21	Colombia	Paper: https://www.so-ups.ru/functioning/ees/ees-2020/
22	Qatar	Personal collaboration
23	India	https://posoco.in/reports/electricity-demand-pattern-analysis/
24	Thailand	http://www.eppo.go.th/index.php/en/en-energystatistics/electricity-statistic
25	Morocco	Report: 'The Moroccan Solar Plan A comparative analysis of CSP and PV utilization until 2020'
26	Saudi Arabia	https://www.ecra.gov.sa/en-us/MediaCenter/doclib2/Pages/SubCategoryList.aspx?categoryID=5
27	Egypt	http://www.moee.gov.eg/english_new/report.aspx
28	Tanzania	Report: 'power system master plan in dar es salaam'
29	Jordan	Paper: https://energsustainsoc.biomedcentral.com/articles/10.1186/s13705-019-0224-1
30	Mozambique	Report: 'Integrated Master Plan Mozambique Power System Development'
31	Ethiopia	Thesis: http://etd.aau.edu.et/handle/123456789/15779
32	West Africa	Paper: https://www.sciencedirect.com/science/article/abs/pii/S0306261919304684

Note: 1) Row 1 ~ 6 list the sources of monthly hydro generation, Row 7 ~ 22 list the sources of historical full year hourly demand, Row 23 ~ 32 list the sources of typical hourly demand. 2) Four countries in West Africa are considered: Ghana, Mali, Niger, Nigeria.

TABLE 16. Regional financial assumptions for technologies and operational parameters.

Technology	Financial assumptions				Limit
	Item	Unit	2030	2040	min, max
Utility PV	Capital	$/kW	321	238	0, 1
	O&M fix	%/year	2.33	2.45	
	O&M var	$/kWh	0	0	
	Lifetime	year	30	30	
Onshore	Capital	$/kW	1075	950	0,1
	O&M fix	%/year	1.90	1.90	
	O&M var	$/kWh	0	0	
	Lifetime	year	25	25	
Offshore	Capital	$/kW	2450	2275	0, 1
	O&M fix	%/year	2.80	2.80	
	O&M var	$/kWh	0	0	
	Lifetime	year	25	25	
Hydro	Capital	$/kW	1704	1704	0, 1
	O&M fix	%/year	1.50	1.50	
	O&M var	$/MWh	5.83	5.83	
	Lifetime	year	40	40	
Li-Battery	Capital	$/kWh	137	93	0, 1; Efficie
	O&M fix	%/year	2.31	2.75	-ncy:0.95; Energy-
	O&M var	$/MWh	0.23	0.23	to-power: 4h
	Lifetime	year	15	15	

Note: 1) The financial assumptions for 2040 were fed to the optimization in this study, similar to [31]. 2) All the regions are assumed to share the same assumptions. 3) The installed cost of hydro power is the weighted average in 2019 from IRENA and assumed to be unchanged in the future.

with higher CF of RE generation, thus serving as generation bases.

As in Fig.5(a), when energy storage is not considered for Case 12, the utilization of solar PV power is thus limited and 'RU_East' becomes an additional generating base instead of mainly the role as an electricity exchange hub between Asia and North America. This shows less need for 'Asia_E' to be connected with North America via long distance

TABLE 17. Regional expected installations in 2030, installed potentials and annual demand in 2050.

Region	Expected installations in 2030 (GW)				Maximum installing potential (GW)				Demand
	onshore	offshore	solar	hydro	onshore	offshore	solar	hydro	(TWh)
EU_Plus	255	72	270	139	1,980	1,167	24,293	334	4,216
RU_WestPlus	12	0	11	28	2,678	833	32,861	179	1,222
RU_East	2	0	0	46	4,526	4,997	55,531	262	313
Middle_East	80	0	140	53	4,788	486	58,743	205	3,771
Asia_C	8	0	6	16	1,831	0	22,471	199	261
Asia_S	188	3	198	92	1,647	278	20,213	327	6,660
Asia_E	453	52	487	475	4,646	754	57,002	658	14,532
Asia_SE	15	0.37	58	103	1,917	1,600	23,522	393	3,643
Oceania	19	0	36	13	3,077	1,187	37,752	57	370
Sub_Saharan	31	0	24	93	9,272	432	113,768	354	2,595
N_America_W	130	1	55	90	1,843	51	22,617	142	1,105
N_America_E	223	41	112	72	3,081	973	37,798	124	5,204
N_America_NE	10	2	3	62	1,115	395	13,680	181	458
S_America	44	0	15	183	7,183	1,087	88,141	597	2,260

Note: 1) The potential of hydro power is originally expressed in unit of 'TWh/year' and is then converted to 'GW' based on the annual CF (2019) from Hydropower Status Report released by IHA; 2) The regional demand has accounted for the transmission & distribution loss

links when wind energy becomes the major supply sources locally.

The annual cumulative electricity flows for other cases are illustrated respectively in Fig.6.

It is obvious that solar power is the major source in 'Asia_E' and in regions of North America for Case 9 in Fig. 6(a) and for Case 5 in Fig. 6(b) and solar power is also the major source for base Case 8 in Fig. 5(b) according to the proposed installation capacities in Table 6. It is shown in those three cases that the annual net import of electricity in 'RU_E' (purple) is small although there are much in-flow and out-flow, indicating that much electricity interaction occurs between 'Asia_E' and North America.

In contrast, when wind energy becomes the major supply sources locally, such as Case 10 in Fig. 6(c) and Case 6 in Fig. 6(d) as well as Case 12 in Fig. 5(a), 'RU_E' is dominated by out-flow (purple) and acts as generation base, indicating there is much less need for 'Asia_E' to be connected with North America via long-distance link.

Above comparison analyses suggest that solar power is the major drive for long distance transmission due to the much time difference and thus stronger solar complementarity.

V. CONCLUSION

This study has investigated the electricity interconnection benefits of 100% RE-sourced global power grid with 14 regions and 20 potential routes by comprehensively comparing 24 supplying portfolios of wind, solar, hydro power, storage system, and load curtailment, based on a co-optimized planning and full year dispatch model where a much stricter '*N*-1' criterion is incorporated. The main conclusions are presented as follows:

1) Global electricity interconnection will yield a minimum saving of 20% of the annual cost for all supply portfolios of 'RE sources + Storage system' under the load curtailment factor of 5% but without load curtailment this increases slightly to 21%. A load curtailment of 5% hardly influences the annual cost for cases with interconnections, indicating less need for load curtailing after the interconnection.
2) For the optimal case with interconnectors, the total capacity of energy storage is around 50% less than that of the reference case without interconnectors, and this indicates that global interconnected electricity grid can bring equivalent energy storage capacity by exploring the complementary characteristics of RE sources particularly solar energy with time differences. This also implies that a global electricity grid can bring significant flexibility while the impact of load curtailment is small.
3) When the complementarity between local RE sources is exploited, e.g., 'PV+Wind+Hydro', the interconnected case performs slightly better than the storage system with a cost decrease of 4% under a load curtailment of 5% and by 2% without load curtailment. Additionally, no load curtailment will increase the annual cost by at least 4% for portfolios of 'RE sources + Interconnection' or 2% for 'RE sources + Storage system'.
4) It has been shown that the time difference based solar complementarity plays a pivotal role in encouraging long distance interconnection. For instance, it is evidenced that there is less need for 'Asia_E' to be connected with North America via long-distance links when wind energy acts as local major supplying sources. In contrast, there is a strong incentive to connect the two regions when solar power becomes the major energy contributor locally due to the 12-hour time difference and thus the maximum solar complementarity can be expected.
5) A much stricter '*N*-1' security criterion than the traditional one has been investigated for the interconnectors between the 14 regions, which allows an outage of any DC line of each interconnection route anytime under all the operating conditions. Interestingly such a '*N*-1' security criterion makes only a small contribution of less than 1% to the total annual system costs.

6) All the deployed interconnectors have an annual UF greater than 30% and annual UFs for 15 interconnectors and 5 interconnectors are more than 40% and 60%, respectively. Additionally, the power flows of the interconnectors change dynamically over a wide range during a week, showing the market value of the links.
7) This paper has carried out a comprehensive economic assessment of the concept of a global electricity grid with 100% RE generation, and it has shown that the economics of interconnection brings significant cost benefits particularly as the energy sources move towards being 100% renewable. This opens up a new pathway to share the temporally and geographically diversified renewable generation sources from a global view and hence implement the net-zero targets efficiently.

APPENDIX

See Tables 15–17.

REFERENCES

[1] *Global Energy Transformation: A Roadmap to 2050*, IRENA, Abu Dhabi, United Arab Emirates, 2019.
[2] M. Z. Jacobson, M. A. Delucchi, M. A. Cameron, S. J. Coughlin, C. A. Hay, I. P. Manogaran, Y. Shu, and A.-K. von Krauland, "Impacts of green new deal energy plans on grid stability, costs, jobs, health, and climate in 143 countries," *One Earth*, vol. 1, no. 4, pp. 449–463, Dec. 2019.
[3] E. Larson, C. Greig, J. Jenkins, and E. Mayfield, *Net Zero America: Potential Pathways, Infrastructure, and Impacts*. rinceton, NJ, USA: Princeton Univ., 2020.
[4] D. Bogdanov, J. Farfan, K. Sadovskaia, A. Aghahosseini, M. Child, A. Gulagi, A. S. Oyewo, L. de Souza Noel Simas Barbosa, and C. Breyer, "Radical transformation pathway towards sustainable electricity via evolutionary steps," *Nature Commun.*, vol. 10, no. 1, pp. 1–16, Dec. 2019.
[5] J. Jurasz, F. A. Canales, A. Kies, M. Guezgouz, and A. Beluco, "A review on the complementarity of renewable energy sources: Concept, metrics, application and future research directions," *Sol. Energy*, vol. 195, pp. 703–724, Jan. 2020.
[6] C. Frank, S. Fiedler, and S. Crewell, "Balancing potential of natural variability and extremes in photovoltaic and wind energy production for European countries," *Renew. Energy*, vol. 163, pp. 674–684, Jan. 2021.
[7] W. A. Braff, J. M. Mueller, and J. E. Trancik, "Value of storage technologies for wind and solar energy," *Nature Climate Change*, vol. 6, p. 964, Oct. 2016.
[8] D. Connolly, H. Lund, and B. V. Mathiesen, "Smart energy europe: The technical and economic impact of one potential 100% renewable energy scenario for the European union," *Renew. Sustain. Energy Rev.*, vol. 60, pp. 1634–1653, Jul. 2016.
[9] P. Sterchele, K. Kersten, A. Palzer, J. Hentschel, and H.-M. Henning, "Assessment of flexible electric vehicle charging in a sector coupling energy system model—Modelling approach and case study," *Appl. Energy*, vol. 258, Jan. 2020, Art. no. 114101.
[10] M. R. M. Cruz, D. Z. Fitiwi, S. F. Santos, and J. P. S. Catalão, "A comprehensive survey of flexibility options for supporting the low-carbon energy future," *Renew. Sustain. Energy Rev.*, vol. 97, pp. 338–353, Dec. 2018.
[11] Y. Shu and W. Chen, "Research and application of UHV power transmission in China," *High Voltage*, vol. 3, no. 1, pp. 1–13, 2018.
[12] X. Zhao, Y. Liu, J. Wu, J. Xiao, J. Hou, J. Gao, and L. Zhong, "Technical and economic demands of HVDC submarine cable technology for global energy interconnection," *Global Energy Interconnection*, vol. 3, no. 2, pp. 120–127, Apr. 2020.
[13] Z. Q. Zhao, Y. M. Dai, X. F. Song, L. C. Sun, and H. Z. Nie, "Research on the economy of UHVDC transmission under the background of global energy interconnect," *IOP Conf. Ser., Mater. Sci. Eng.*, vol. 439, no. 5, 2018, Art. no. 052022.
[14] S. Chatzivasileiadis, D. Ernst, and G. Andersson, "The global grid," *Renew. Energy*, vol. 57, pp. 372–383, Sep. 2013.
[15] Z. Liu, *Global Energy Interconnection*. Amsterdam, The Netherlands: Elsevier, 2015.
[16] A. Boute and P. Willems, "RUSTEC: Greening Europe's energy supply by developing Russia's renewable energy potential," *Energy Policy*, vol. 51, pp. 618–629, Dec. 2012.
[17] F. Zickfeld, A. Wieland, J. Blohmke, M. Sohm, A. Yousef, M. Pudlik, M. Ragwitz, and F. Sensfuß, "Desert power 2050: Perspectives on a sustainable power system for EUMENA," Dii GmbH, Munich, Germany, Tech. Rep., 2012. [Online]. Available: http://www.desertec-uk.org.uk/reports/DII/DPP_2050_Study.pdf
[18] M. Ardelean and P. Minnebo, *A China-EU Electricity Transmission Link: Assessment of Potential Connecting Countries and Routes*. Ispra, Italy: Joint Research Center (JRC), 2017.
[19] M. Ardelean, P. Minnebo, and H. Gerbelová, "Optimal paths for electricity interconnections between Central Asia and Europe," Joint Res. Center, Luxembourg, Tech. Rep. EUR 30156 EN, 2020.
[20] A. Purvins, L. Sereno, M. Ardelean, C.-F. Covrig, T. Efthimiadis, and P. Minnebo, "Submarine power cable between Europe and North America: A techno-economic analysis," *J. Cleaner Prod.*, vol. 186, pp. 131–145, Jun. 2018.
[21] C. Huang, C. Wang, H. Li, J. Luo, W. Sun, and X. Du, "Analysis of basic conditions of the power grid interconnection among Xinjiang, Pakistan, and five central Asian countries," *Global Energy Interconnection*, vol. 2, no. 1, pp. 54–63, Feb. 2019.
[22] X. Junrong, W. Chun, X. Xiaohui, and L. Chaoqun, "Renewable energy generation linked by future China-Arab interconnection," (in Chinese), *Power Syst. Technol.*, vol. 40, no. 12, p. 9, 2016.
[23] GEIDCO. (2018). *Global Energy Interconnection Backbone Grid Research*. [Online]. Available: http://globalsmartgridfederation.org/page/480/world-global-energy-interconnection-backbone-grid-research
[24] *China's Grid Architect Proposes a Made in China Upgrade to North America's Power System*. Accessed: Sep. 2019. [Online]. Available: https://spectrum.ieee.org/energywise/energy/renewables/chinas-grid-architect-offers-made-in-china-upgrade-to-north-americas-power-system
[25] *EuroAsia Interconnector*. Accessed: Oct. 2019. [Online]. Available: https://www.euroasia-interconnector.com/
[26] A. Bloom, J. Novacheck, G. Brinkman, and J. McCalley, *The Value of Increased HVDC Capacity Between Eastern and Western U.S. Grids: The Interconnections Seam Study*. Golden, CO, USA: NREL, 2020.
[27] R. B. Fuller and K. Kuromiya, *Critical Path*. New York, NY, USA: Macmillan, 1981.
[28] M. Brinkerink, B. Ó. Gallachóir, and P. Deane, "A comprehensive review on the benefits and challenges of global power grids and intercontinental interconnectors," *Renew. Sustain. Energy Rev.*, vol. 107, pp. 274–287, Jun. 2019.
[29] J. Yu, K. Bakic, A. Kumar, A. Iliceto, L. B. Tabu, J. L. Ruaud, J. Fan, B. Cova, H. Li, D. Ernst, and R. Fonteneau, "Global electricity network-feasibility study," CIGRE, Paris, France, Tech. Rep. TB775, 2019.
[30] K. Hansen, C. Breyer, and H. Lund, "Status and perspectives on 100% renewable energy systems," *Energy*, vol. 175, pp. 471–480, May 2019.
[31] W. Zappa, M. Junginger, and M. van den Broek, "Is a 100% renewable European power system feasible by 2050?" *Appl. Energy*, vols. 233–234, pp. 1027–1050, Jan. 2019.
[32] D. P. Schlachtberger, T. Brown, S. Schramm, and M. Greiner, "The benefits of cooperation in a highly renewable European electricity network," *Energy*, vol. 134, pp. 469–481, Sep. 2017.
[33] D. Bogdanov and C. Breyer, "North-East Asian super grid for 100% renewable energy supply: Optimal mix of energy technologies for electricity, gas and heat supply options," *Energy Convers. Manage.*, vol. 112, pp. 176–190, Mar. 2016.
[34] A. Aghahosseini, D. Bogdanov, L. S. N. S. Barbosa, and C. Breyer, "Analysing the feasibility of powering the Americas with renewable energy and inter-regional grid interconnections by 2030," *Renew. Sustain. Energy Rev.*, vol. 105, pp. 187–205, May 2019.
[35] H. Liu, G. B. Andresen, and M. Greiner, "Cost-optimal design of a simplified highly renewable Chinese electricity network," *Energy*, vol. 147, pp. 534–546, Mar. 2018.
[36] H. Liu, T. Brown, G. B. Andresen, D. P. Schlachtberger, and M. Greiner, "The role of hydro power, storage and transmission in the decarbonization of the Chinese power system," *Appl. Energy*, vol. 239, pp. 1308–1321, Apr. 2019.

[37] P. R. Brown and A. Botterud, "The value of inter-regional coordination and transmission in decarbonizing the US electricity system," *Joule*, vol. 5, no. 1, pp. 115–134, Jan. 2021.
[38] C. Wu, X.-P. Zhang, and M. J. H. Sterling, "Economic analysis of power grid interconnections among Europe, North-East Asia, and North America with 100% renewable energy generation," *IEEE Open Access J. Power Energy*, vol. 8, pp. 268–280, 2021.
[39] G. B. Andresen, A. A. Søndergaard, and M. Greiner, "Validation of Danish wind time series from a new global renewable energy atlas for energy system analysis," *Energy*, vol. 93, pp. 1074–1088, Dec. 2015.
[40] J. Hörsch, F. Hofmann, D. Schlachtberger, and T. Brown, "PyPSA-eur: An open optimisation model of the European transmission system," *Energy Strategy Rev.*, vol. 22, pp. 207–215, Nov. 2018.
[41] OEP. *Wind Turbine Library*. Accessed: May 2020. [Online]. Available: https://openenergy-platform.org/dataedit/view/supply/wind_turbine_library
[42] *Optimum Tilt of Solar Panels*. Accessed: May 2020. [Online]. Available: http://www.solarpaneltilt.com/#fixed
[43] S. Beringer, H. Schilke, I. Lohse, and G. Seckmeyer, "Case study showing that the tilt angle of photovoltaic plants is nearly irrelevant," *Sol. Energy*, vol. 85, no. 3, pp. 470–476, Mar. 2011.
[44] X. M. Chen, Y. Li, B. Y. Zhao, and R. Z. Wang, "Are the optimum angles of photovoltaic systems so important?" *Renew. Sustain. Energy Rev.*, vol. 124, May 2020, Art. no. 109791.
[45] T. Huld, R. Gottschalg, H. G. Beyer, and M. Topič, "Mapping the performance of PV modules, effects of module type and data averaging," *Sol. Energy*, vol. 84, no. 2, pp. 324–338, Feb. 2010.
[46] S. Pfenninger and I. Staffell, "Long-term patterns of European PV output using 30 years of validated hourly reanalysis and satellite data," *Energy*, vol. 114, pp. 1251–1265, Nov. 2016.
[47] E. Schubert, J. Sander, M. Ester, H. P. Kriegel, and X. Xu, "DBSCAN revisited, revisited: Why and how you should (still) use DBSCAN," *ACM Trans. Database Syst.*, vol. 42, no. 3, pp. 1–21, 2017.
[48] *Monthly Electricity Statistics*. Accessed: Mar. 2021. [Online]. Available: https://www.iea.org/reports/monthly-electricity-statistics
[49] *Hydropower Status Report*, International Hydropower Association, London, U.K., 2020.
[50] *2010 Survey of Energy Resources*, World Energy Council, London, U.K., 2010.
[51] E. Vartiainen, G. Masson, C. Breyer, D. Moser, and E. R. Medina, "Impact of weighted average cost of capital, capital expenditure, and other parameters on future utility-scale PV levelised cost of electricity," *Prog. Photovolt., Res. Appl.*, vol. 28, no. 6, pp. 439–453, Jun. 2020.
[52] *Renewable Power Generation Costs in 2019*, IRENA, Abu Dhabi, United Arab Emirates, 2020.
[53] *Future of WiND: Deployment, Investment Technology, Grid Integration and Socio-Economic Aspects*, IRENA, Abu Dhabi, United Arab Emirates, 2019
[54] *Future of Solar: Deployment, Investment Technology, Grid Integration and Socio-Economic Aspects*, IRENA, Abu Dhabi, United Arab Emirates, 2019.
[55] *Cost Projections for Utility-Scale Battery Storage*, NREL, Golden, CO, USA, 2019.
[56] *Grid Energy Storage Technology Cost and Performance Assessment*, DoE, United States Department of Energy, Washington, DC, USA, 2020.
[57] *Welcome to Balancing Services*. Accessed: Apr. 2021. [Online]. Available: https://www.nationalgrideso.com/industry-information/balancing-services

CONG WU received the B.Eng. and M.Sc. degrees in electrical engineering from China Agricultural University, Beijing, China, in 2015 and 2017, respectively, and the Ph.D. degree in electrical engineering from the University of Birmingham, Birmingham, U.K., in 2021. His research interests include transcontinental electricity interconnection, power system planning, and optimal power flow.

XIAO-PING ZHANG (Fellow, IEEE) is currently a Professor of electrical power systems with the University of Birmingham, U.K. He is also the Director of Smart Grid with Birmingham Energy Institute and the Co-Director of the Birmingham Energy Storage Center. He has coauthored the first and second edition of the monograph *Flexible AC Transmission Systems: Modeling and Control* (Springer), in 2006 and 2012. He has also coauthored the book *Restructured Electric Power Systems: Analysis of Electricity Markets with Equilibrium Models* (IEEE Press/Wiley), in 2010. His research interests include modeling and control of HVDC, FACTS, and wind/wave generation, distributed energy systems and market operations, and power system planning. He has been made a fellow of IEEE for contributions to modeling and control of high-voltage DC and AC transmission systems. He is an IEEE PES Distinguished Lecturer on HVDC, FACTS, and Wave Energy Generation. He is also a fellow of IET. He has been an Advisor to IEEE PES U.K. and Ireland Chapter and chairing the IEEE PES WG on Test Systems for Economic Analysis. He has been appointed recently to the Expert Advisory Group of U.K. Government's Offshore Transmission Network Review.

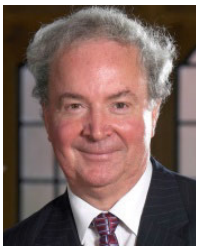

MICHAEL J. H. STERLING received the B.Eng. degree (Hons.) in electronic and electrical engineering from the University of Sheffield, U.K., in 1968, the Ph.D. degree in computer control of power systems, in 1971, and the D.Eng. degree, in 1988. In 1971, he joined the Department of Control Engineering, University of Sheffield, as a Lecturer, where he was promoted to a Senior Lecturer, in 1978. In 1980, he was appointed as a Professor with the University of Durham, U.K., before being appointed the Vice-Chancellor and the Principal of Brunel University, in 1990. He subsequently became the Vice-Chancellor of the University of Birmingham, in 2001. He retired as one of the U.K.'s longest-serving University Leaders, in 2009. He is a fellow of the Institution of Engineering and Technology, the Institute of Measurement and Control, and the Royal Academy of Engineering. He was a member of the U.K. Prime Minister's Council for Science and Technology from 2003 to 2013, where he was also the Chair of the Energy Group. He served as the Chairman for many organizations, most recently the Science and Technology Facilities Council (2009–2018).